Thermal Behavior and Characterization of Some 2-Oxazolidinone Derivatives[1)]

Choichiro SHIMASAKI,* Shuichi HAYASE, Atsuko MURAI, Junko TAKAI, Eiichi TSUKURIMICHI, and Toshiaki YOSHIMURA
Faculty of Engineering, Toyama University, Gofuku, Toyama-shi 930
(Received October 30, 1989)

Four kinds of 2-oxazolidinone derivatives, (**1**) [5-phenoxymethyl-3-phenylcarbamoyl-2-oxazolidinone (**1a**), 2,4-bis(2-oxo-3-oxazolidin-3-ylcarbonylamino)toluene (**1b**), *N,N'*-bis(2-oxo-3-oxazolidin-3-ylcarbonyl)-1,6-hexanediamine (**1c**), and 1,4-bis(3-phenylcarbamoyl-2-oxo-5-oxazolidin-5-ylmethoxy)benzene (**1d**)], were prepared with the addition of 2-oxazolidinone, 5-phenoxymethyl-2-oxazolidinone (**2**), and 1,4-bis(2-oxo-5-oxazolidin-5-ylmethoxy)benzene (**3**) to mono- or diisocyanates by using *N,N*-dimethylformamide or benzene as solvents and 1,4-diazabicyclo[2.2.2]octane as a catalyst. Compound **1** was found to be thermally stable by thermal analysis. DSC curves of these compounds revealed an endothermic peak due to melting, except for **1d** which was obtained from **3**. The main fragmentation mechanism by electron impact for **1** was found to consist of two processes: simple cleavage and a rearrangement reaction. Further, each process was followed by cleavage modes. The proportion of fragment ions containing the benzene ring in the main fragmentation was greater than 80%. From the DTA-TG/DTG curves, the difference between EI-cleavage and thermal decomposition for **1a** was elucidated.

Linear macromolecules with a pendant 2-oxazolidinone ring have been extensively investigated.[2)] However the polymers containing 2-oxazolidinone rings in their main chains have scarcely been investigated, probably because of experimental difficulties. Recently, Ishikawa et al.[3)] developed a new synthetic method for the 2-oxazolidinone derivatives (**1**). Four kinds of **1** were synthesized with the addition of 2-oxazolidinone, 5-phenoxymethyl-2-oxazolidinone (**2**), and 1,4-bis(2-oxo-5-oxazolidin-5-ylmethoxy)benzene (**3**) to mono- or diisocyanates. Their structual formula are shown below.

Thermal analysis has been used mainly to examine the thermal behavior of these compounds. In the present study, the pyrolysis process for these compounds was examined in order to carry out further studies for the application of **2** as a thermally stable plasticizer. Both ^{1}H or ^{13}C NMR and mass spectroscopy were used to determine the structure and the main fragmentation by electron impact. The pyrolysis mechanism is also discussed.

Experimental

Materials. All chemicals were of analytical grade and were used without further purification. Compound **2** was prepared as described by Henkel.[4)] Compound **3** was obtained by reacting tris(2,3-epoxypropyl)isocyanurate with hydroquinone in the presence of an alkali catalyst.[1,3)] Compounds **2** and **3** were recrystallized twice in water and an acid medium of glacial acetic acid.

Preparation of Compounds. All compounds were prepared by methods described in the literature,[3)] or analogous methods. By way of example, **1d** was synthesized by the following method. Compound **3** (2.0 g), phenyl isocyanate (1.5 g), and 1,4-diazabicyclo[2.2.2]octane(0.14 g) were dissolved in 30 ml *N,N*-dimethylformamide; the mixture was reacted under nitrogen atmosphere at 90 °C for six hours. The filtrate was distilled under reduced pressure, and the soluble residue was removed by extraction with small quantities of ethanol. Compound **1d** was further purified by crystallization twice from *N,N*-dimethylformamide–water (1 : 1). Compounds **2** and **3** were prepared by a reaction of tris(2,3-epoxypropyl)isocyanurate with phenol and hydro-

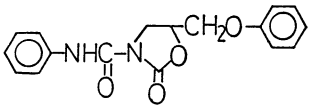

1a 5-Phenoxymethyl-3-phenylcarbamoyl-2-oxazolidinone

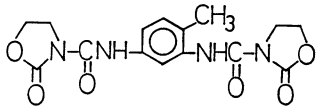

1b 2,4-Bis(2-oxo-3-oxazolidin-3-ylcarbonylamino)toluene

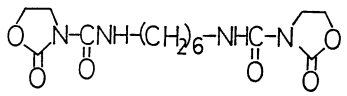

1c N,N'-Bis(2-oxo-3-oxazolidin-3-ylcarbonyl)-1,6-hexanediamine

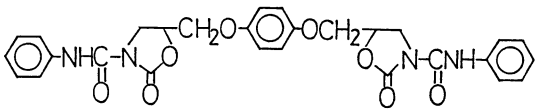

1d 1,4-Bis(3-phenylcarbamoyl-2-oxo-5-oxazolidin-5-ylmethoxy)benzene

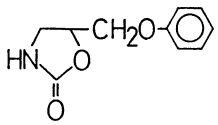

2 5-phenoxymethyl-2-oxazolidinone

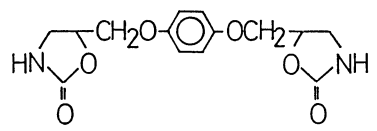

3 1,4-bis(2-oxo-5-oxazolidin-5-ylmethoxy)benzene

Chemical Formula.

Table 1. Physical Properties of **1a**, **1b**, **1c**, and **1d**

		Compound			
		1a	**1b**	**1c**	**1d**
Formula (Mol. wt.)		$C_{17}H_{16}N_2O_4$ (312.33)	$C_{15}H_{16}N_4O_6$ (348.31)	$C_{14}H_{22}N_4O_6$ (342.35)	$C_{28}H_{26}N_4O_8$ (546.52)
Elemental analysis	C	65.29 (65.38)	52.42 (51.72)	49.21 (49.11)	60.33 (61.53)
Found (Calcd)/%	H	5.21 (5.16)	4.72 (4.63)	6.53 (6.48)	4.97 (4.80)
	N	8.96 (8.97)	15.62 (16.09)	16.22 (16.37)	10.24 (10.25)
Melting point/ °C		141.9—144.5	206.0—207.0	126.0—128.5	210.0—220.0
IR spectra/cm^{-1}	$\nu_{C=O}$	1765	1740	1745	1745
	ν_{NH}	3240	3260	3350	3260
Mass spectra (70 eV, m/z M^+)		312	348	342	(308)[a]

a) The M^+ is not detectable and the value in parentheses indicates the maximum m/z.

quinone in the presence of sodium hydroxide as a catalyst in a refluxing solution of *N,N*-dimethylformamide. As shown in Table 1, the purity of the compounds was checked by elemental analyses of carbon, hydrogen, and nitrogen and by IR and/or NMR.

Measurements. Thermal analysis was performed by using a Rigaku Denki TG-DTA and TG-DSC apparatus in air at a heating rate of 5 °C min^{-1}. TG-TRAP-GC/MS and TG-MS were carried out with the Shimadzu combined system in stationary helium gas at a heating rate of 10 °C min^{-1}. The IR spectrum was recorded on an Nihon Bunko IR-810 using the KBr-disc method. The mass spectrum was taken with an ionization potential of between 20 and 70 eV using a JEOL-JMS-D300. The ^1H and ^{13}C NMR spectra were obtained at room temperature for a chloroform-*d* and dimethyl-d_6 sulfoxide solution containing 1% tetramethylsilane (TMS) as the internal standard. A JNM-FX 90, Fourier transform spectrometer was used for the measurement of ^1H and ^{13}C NMR, respectively.

The melting points were determined on a Mitamura micromelting apparatus without correction. Preparative TLC was carried out on silica gel (Kieselgel 60, Merck A. G., Darmstadt). Elemental analysis was performed by the Analytical Center at the Faculty of Pharaceutical Science at Toyama Medical and Pharmaceutical University.

Results and Discussion

Thermal Analysis. Figure 1 shows the DSC and TG curves for **1**, as determined at a heating rate 5 °C min^{-1}. The DSC curves for **1a** exhibited two endothermic peaks; for **1b**, **1c**, and **1d** there were three and four endothermic peaks. The second endothermic peak for **1a** and both the second and third for **1b** was due to thermal decomposition; this was confirmed by TG. On the other hand, the DSC curve for **1d** exhibited four endothermic peaks. The first three peaks comprise two melting points with a transition. The

Table 2. Heat of Fusion of **1**

Compound		Mp/ °C[a]	Heat of fusion /kJ mol^{-1}
1a		142.7	12.9
1b		206.3	5.2
1c		127.6	8.9
1d	Form-I	202.0	10.1
	Form-II	229.0	5.1

a) DSC peak temperature.

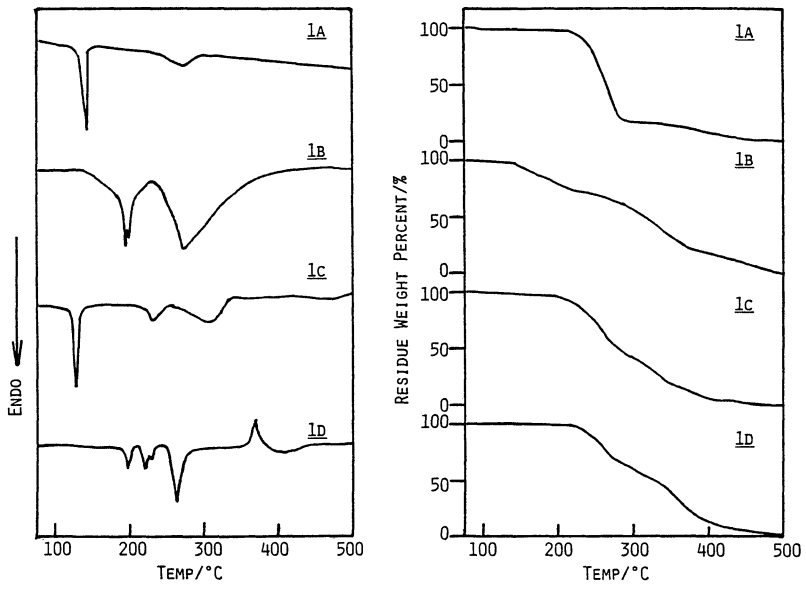

Fig. 1. DSC and TG curves of **1**.

fourth peak is due to thermal decomposition. The TG curves show that the pyrolysis process for **1a** take places in one stage and for **1b**, **1c**, and **1d** in two stages. The heat of fusion for **1** was evaluated as shown in Table 2.

The problem is now discussed from a slightly different point of view. The DSC measurements of the first three peaks for **1d** are carried out by the following three methods in which the samples are sealed in an aluminum pan:

A) The powder sample was firmly loaded into an aluminum pan and then hermetically sealed with a jack.

B) The powder sample was firmly loaded into an aluminum pan.

C) The powder sample was lightly loaded with the aid of a special holder into an aluminum pan (the usual packing method).

With an increased packing density the leakage of decomposition gas decreased in method (A). As shown in Fig. 2, the temperature of the thermal decomposition varies with the self-generated atmosphere formed by the decomposition gas because of the decomposition and recombination process. The change in the pressure of the self-generated atmosphere had no influence on the temperatures for the three endothermic peaks.

The heating-cooling cycle process was measured with a DSC apparatus over the temperature range from 30 to 230 °C. In the first process, three endothermic peaks were observed for the DSC curve of **1d**. After the first heating-cooling process, E_{D1} and E_{D2} disappeared and only the E_{D3} peak remained.

The kinetic analysis of the thermal decomposition was carried out according to the Ozawa method.[5] The sample was lightly loaded with the aid of a special holder into an aluminum pan. Thermal decomposition was studied at heating rates of 2.5, 5.0, 10.0, and 20.0 °C min^{-1}. According to the Ozawa theory the weight loss (θ) at constant heating rate is expressed by the following equation:

$$\theta = \Delta E/aR \cdot P(\Delta E/RT), \quad (1)$$

where ΔE is the activation energy, a the heating rate, and R the gas constant. Also, in the case $60 > \Delta E/RT > 20$,

$$\log P(\Delta E/RT) = -\log a - 0.456\Delta E/RT. \quad (2)$$

From plots of the logarithms of the heating rate versus the reciprocal of the absolute temperature for the given residual weight, the activation energy was obtained by the slope of the straight lines. Figure 3 shows plots for **1a**. Linear relationships were also

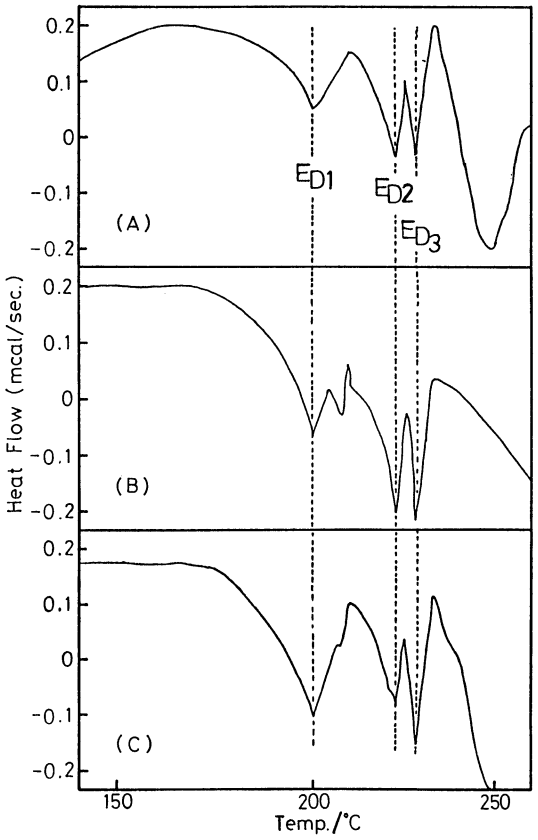

Fig. 2. Effect of different packings on the DSC curve of **1d**.

Table 3. Kinetic Data for the Thermal Decomposition Process of **1**

Compound		ΔE/kJ mol^{-1}	r[a]
1a		138.9	0.999
1b	First stage	260.2	0.935
	Second stage	174.8	0.690
1c		143.5	0.984
1d	First stage	97.8	0.961
	Second stage	148.3	0.985

a) Linear correlation coefficient.

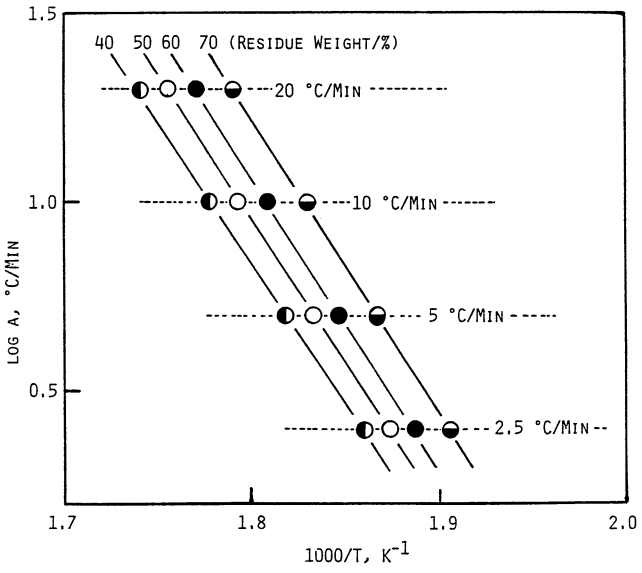

Fig. 3. Plots of logarithms of heating rate versus the reciprocal of absolute temperature for the given conversation of pyrolysis of **1a**.

obtained for **1b**, **1c**, and **1d** during the initial stage of the thermal decomposition process in the TG curve. The results are summarized in Table 3.

Mass Spectra. The thermal decomposition process may be directly predictable from the corresponding mass spectra. Measurements of the mass spectra are the same at from 10 to 75 eV. The low-resolution mass spectra for **1a**, **1b**, **1c**, and **1d** are shown in Fig. 4. These spectra indicate that the M^+ peak is present for all samples, except for **1d**. These observed fragment ions of the low-resolution mass spectra for each compound in Fig. 4 were confirmed by high-resolution mass spectral data for the identification of m/z, its corresponding elemental composition, and the probable molecular structure. The detailed cleavage mechanism for **1**, except **1c**,[1] is unknown at present. The main cleavage mechanism for **1**, except **1c**, is shown in Schemes 1, 2, and 3.

To obtain the relative intensity of the raw peak height of the fragment ion, the ion of largest intensity in the spectrum is selected. The intensity of this ion peak is called the base peak intensity. The base peaks for **1a** and **1d** appeared at m/z 119 due to phenyl isocyanate, for **1b** at m/z 174 due to $(C_9H_6N_2O_2)^+$, and for **1c** at m/z 143 due to $(C_5H_7N_2O_3)^+$. The peaks at m/z 91 and 64 for **1a** and **1d** are the results of the ions from those base peaks.

In Scheme 1, the first process involves the shifting of electrons. After the formation of the M^+ ion at m/z 312, the well-known McLafferty rearrangement leads

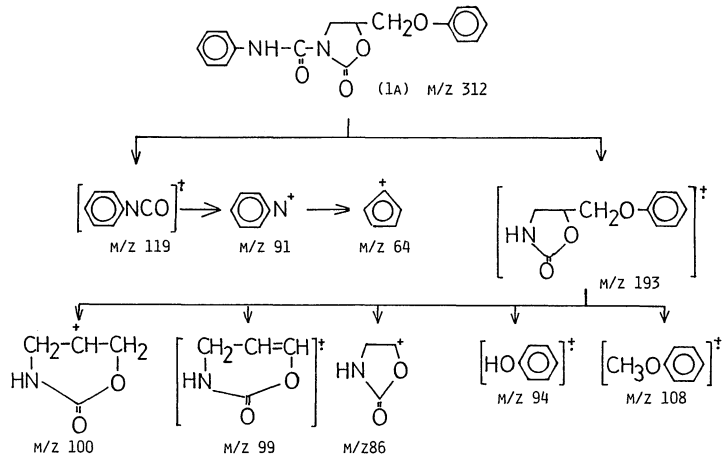

Scheme 1.

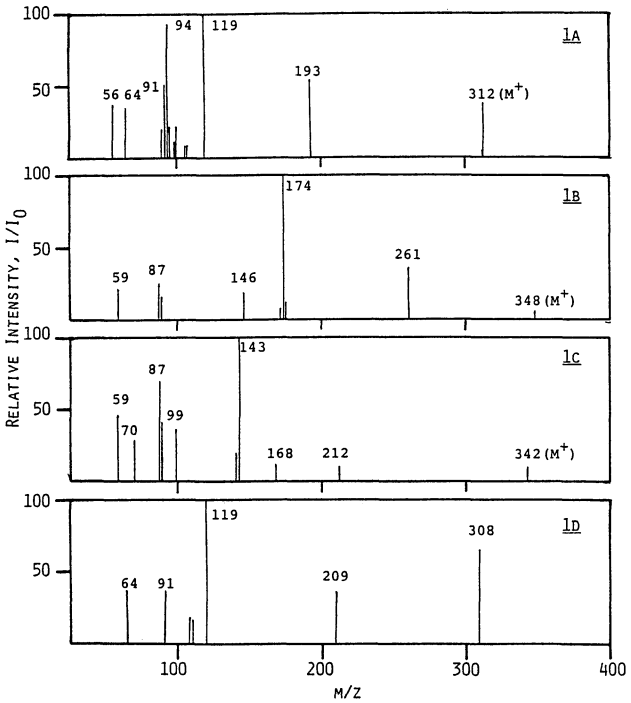

Fig. 4. Low resolution mass spectra (from m/z 50 to 500 at 20 eV.) of **1**.

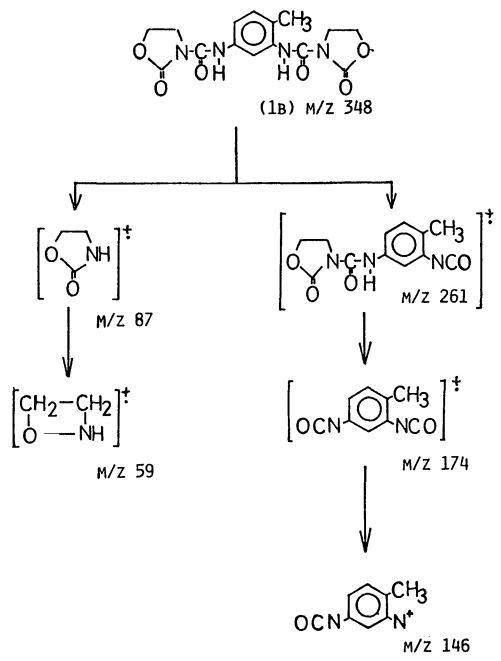

Scheme 2.

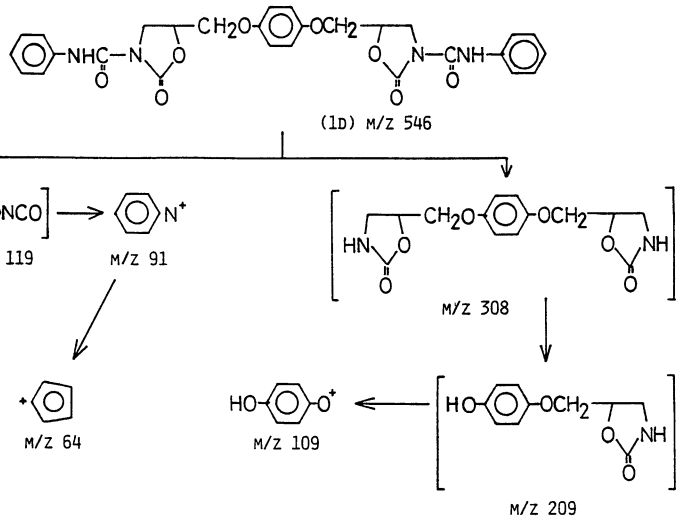

Scheme 3.

to two species at m/z 193 and 119. The former fragment ion splits into many species, such as m/z 86, 94, 99, 100, and 108.

After the formation of the M^+ ion at m/z 348 in Scheme 2, the cleavage of the M^+ ion follows to produce ions at m/z 87 (oxazolidinone) and m/z 261. The former fragment ion leads to the species at m/z 59. The formation of the fragment ion at m/z 261 occured by a McLafferty rearrangement. This fragment ion splits into an ion at m/z 146 via an ion at m/z 174.

As shown in Scheme 3 for **1d**, the intense fragment ion at m/z 308 is characteristic for **3**. After the loss of $C_4H_5NO_2$, the cleavage produces a fragment ion at m/z 209. The simple cleavage of the O-CH_2 bond between the benzene ring and the oxazolidinone ring of this ion leads to a species at m/z 109.

Tandem Thermogravimetric Analyzer-Gas Chromatograph-Mass Spectrometer System. To investigate the thermal decomposition processes which cause the DTA and the TG curves over the range from 200 to 500 °C for **1a**, the TG-TRAP-GC/MS (Method-**A**) and the TG-MS (Method-**B**) were carried out in stationary He. For Method-**B**, the effluent gas from TG was directly introduced into a mass spectrometer. However, in many cases the TG effluent gas was composed of various components. The identification of less abundant components became increasingly difficult. In addition, a quantitative estimation of the constituents is very difficult. Another approach is to collect the pyrolysis products and to then analyze this collected material by GC. This method has been ap-

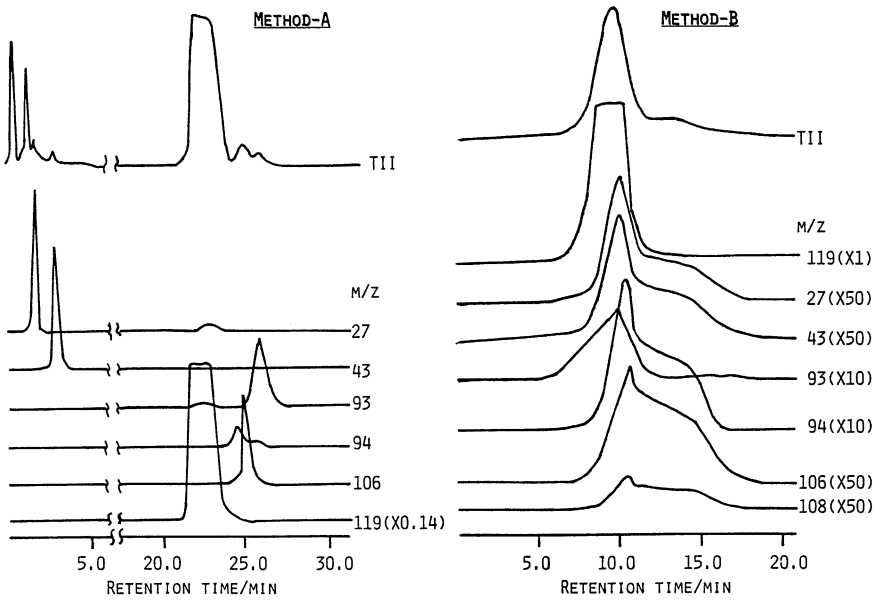

Fig. 5. Mass chromatogram of the decomposition products of **1a** with TG-TRAP-GC/MS (Method-**A**) and TG-MS (Method-**B**).

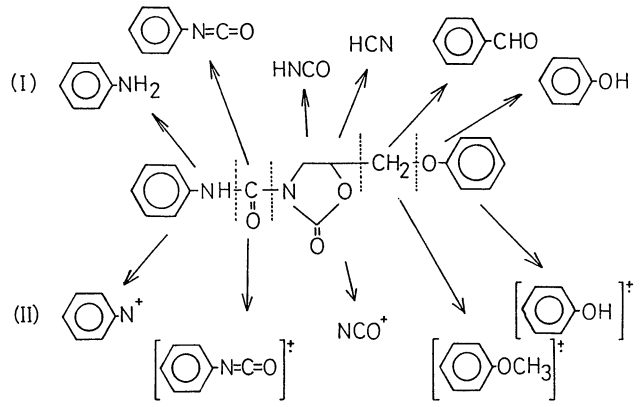

Fig. 6. Chemical species of pyrolysis(I) and main fragment ion by the electron impact(II) for **1a**.

plied to the analysis of thermal degradation products.[6] Figure 5 shows a mass chromatogram of the liberated decomposition products of **1a**, with Method-**A** and **B**, respectively. The thermally degraded products of **1a** from both methods consist of a complex mixture of about six components: HCN, HNCO, $C_6H_5NH_2$, C_6H_5OH, C_6H_5CHO, and C_6H_5NCO. These components were identified by measuring the mass spectrum of the liberated gas from the principal portion of the weight loss on the TG curve between 200 and 250 °C. The peak at *m/z* 119 due to C_6H_5NCO was the most intense. The chemical species of **1a** by thermal decomposition was compared with those of the fragment ions of **1a** by electron impacts (Fig. 6). This figure indicates that the cleavage mechanism between the two degradation processes differs from one another.

We thank Mr. Yoshiharu Yoneyama for the NMR measurements and Miss Misao Shinoda for the Mass spectra. We thank Prof. Shigeya Takeuchi for his good advice regarding the DSC measurements.

References

1) This paper forms Part XIII of "Studies on Decomposition and Formation of Triazine Series Compounds" series. For part XII of this series, see C. Shimasaki, A. Murai, Y. Sakai, and E. Tsukurimichi, *Chem. Lett.*, **1988**, 1009.

2) e.g. T. Endo and M. Okawara, *Makromol. Chem.*, **112**, 49 (1968); T. Endo, R. Numazawa, and M. Okawara, *ibid.*, **123**, 46 (1969), *Bull. Chem. Soc. Jpn.*, **42**, 1101 (1969); W. F. Tousignant and W. E. Walls, U.S. Patent 3133904 (1969).

3) T. Ishikawa and N. Watanabe, *Nippon Kagaku Kaishi*, **1980**, 852.

4) Henkel & Cie. G. m.b.H. Fr. Patent 1487641 (1967).

5) T. Ozawa, *Bull. Chem. Soc. Jpn.*, **38**, 1881 (1965); T. Ozawa, *J. Therm. Anal.*, **2**, 301 (1970).

6) e.g. E. A. Boettner, G. Ball, and B. Weiss, *J. Appl. Polym. Sci.*, **13**, 377 (1969); W. H. Hale, A. G. Farham, R. N. Johnson, and R. A. Clendiving, *J. Polym. Sci., Part-1*, **5**, 2399 (1967); J. Chia, *Thermochim. Acta*, **1**, 231 (1970); J. Chiu, *Anal. Chem.*, **40**, 1516 (1968).